



An innovative agent-based technique for determination of tortuosity in porous materials – Case study: bread and bread dough

Arash Ghaitaranpour^{*}, Mohebbat Mohebbi^{**} , Arash Koocheki

Department of Food Science and Technology, Ferdowsi University of Mashhad, Mashhad, Iran

ARTICLE INFO

Keywords:

Tortuosity
Multi-agent systems
Bread and bread dough
Heat and mass transfer
Image processing

ABSTRACT

Tortuosity is an important structural parameter of porous materials, and it is the ratio of the actual distance between two points to the shortest linear distance between them. In the current work, we illustrate the employment of Brownian motion principles for the estimation of the average tortuosity. Two types of images were used in this work. The first one was standard images with a certain pre-defined direct length and tortuosity, and they were used for the standardization and calibration of our new method of tortuosity measurement. The second one was real images of the cross-sectional view of bread samples during baking. Tortuosity and porosity of bread were tracked at different times of baking. All image types had three connected parts named start section, transmission path region, and end section. In these images, the average tortuosity from start to end section was estimated, using the principle of Brownian motion applied in a multi-agent system. The average tortuosity of bread porous structure during baking was found to be $2-\infty$. In the first stage of baking, tortuosity decreased rapidly, while at the end of this process, the tortuosity of the bread structure increased slightly. Moreover, the effect of porosity and pore distribution pattern on tortuosity could be evaluated easily, and heterogeneity of the desired structure could be illustrated. Therefore, this new method is a valuable technique to measure tortuosity in bakery products and to describe porous materials.

1. Introduction

The behavior of physical phenomena such as fluid flow, heat, and mass transfer at the macroscopic scale is influenced by their microscopic interactions, particularly in porous materials (Ghaitaranpour et al., 2020). Porous media represent an essential type of complex structure, especially in the field of food products (Silva et al., 2015). The pore phase in porous media is complex, with pore size distribution in a wide range. This range is from bakery products such as bread and doughnut with heterogeneous multiscale connected pores and porosity higher than 50% to the other kinds of food products like nuggets with separated pores and porosity less than 50% (Abderrahmene et al., 2017; Ghaitaranpour et al., 2018a,b).

Porous structures are unique in that the paths they provide for the diffusion of particles or the flow of heat and fluid are not straight but tortuous, so the particles, heat or fluid must traverse a longer path (Abderrahmene et al., 2017; Ghaitaranpour et al., 2021). Tortuosity and porosity purely geometrical affect the different types of transfer phenomena in a porous structure. Tortuosity is a concept used to describe

the structure of porous media, estimate their electrical and hydraulic conductivity, and analyze tracer dispersion in terms of travel time and length. However, various types of tortuosity-geometric, hydraulic, electrical, and diffusive-have often been used interchangeably in the literature. In this study, our focus is on determining mean geometric tortuosity (Abderrahmene et al., 2017; Ghanbarian et al., 2013; Kuruneru et al., 2017). Geometric tortuosity is a term employed to describe the amount of increase in the distance of a diffusing molecule movement between two points because of the twisting and diverging of the pore phase in porous structures. A straight line has a tortuosity of precisely one, whereas a line's tortuosity going through a particle bed of the same size beads is about 2 and 3 (Martin, 1993; San Wu, van Vliet, Frijlink and van der Voort Maarschalk, 2006; Zare and Hashemabadi, 2019). Based on the explanation of geometric tortuosity, it is generally described as following specific ratio (the shortest path length to the Euclidean distance between two points) as shown in equation (1)

$$\tau = \frac{L_R}{L_{sh}} \quad (1)$$

^{*} Corresponding author.

^{**} Corresponding author.

E-mail addresses: ghaitaranpour@gmail.com (A. Ghaitaranpour), mohebbatm@gmail.com, m-mohebbi@um.ac.ir (M. Mohebbi).

<https://doi.org/10.1016/j.crf.2025.100995>

Received 9 October 2024; Received in revised form 29 January 2025; Accepted 30 January 2025

Available online 21 February 2025

2665-9271/© 2025 Published by Elsevier B.V. This is an open access article under the CC BY-NC-ND license (<http://creativecommons.org/licenses/by-nc-nd/4.0/>).

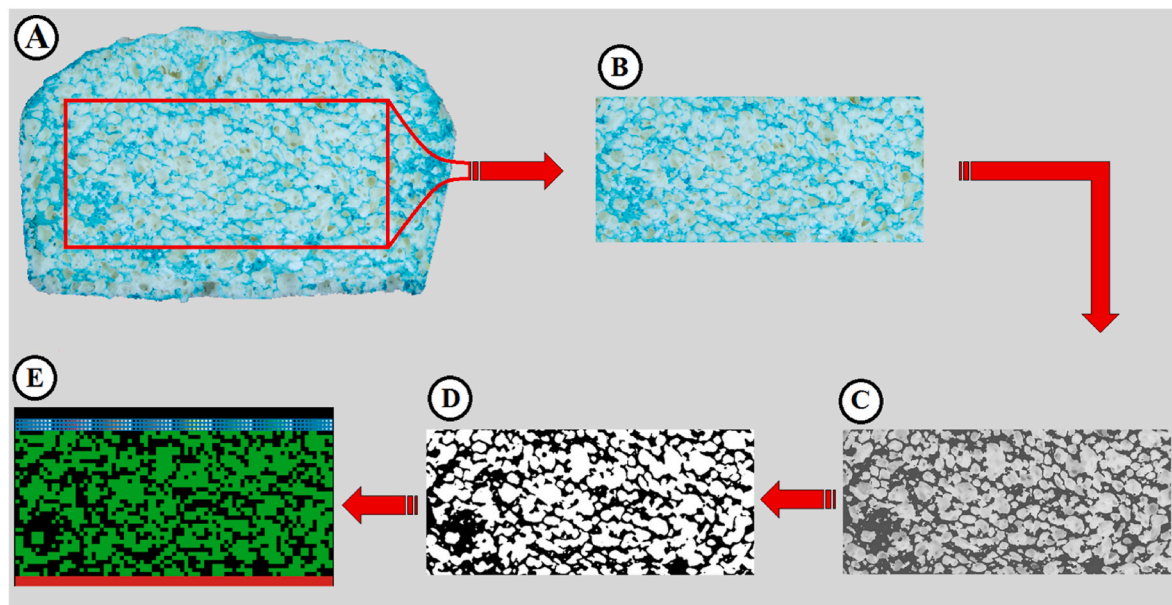


Fig. 1. A & B: Painted cross-section of Bread, C: 8-byte form of bread image, D: 2-byte form of bread image, E: bread structure in Netlogo platform.

In which τ is the tortuosity, L_R is the length of the shortest path through the pores phase, and L_{sh} is the direct distance between two ends of the path (Zare and Hashemabadi, 2019).

Several methods estimate a materials' tortuosity (Huang et al., 2019; Shen and Chen, 2007). It should be mentioned that 2D tortuosity is a qualitative descriptor and not necessarily related to transport in 3D samples (Besbes et al., 2013). A usual way to estimate the 2D tortuosity is through image analysis techniques. Image analysis has become an essential technique of quantifying porous structures' transport and structural characteristics lately (Tranter et al., 2019). One of the most powerful material features is tortuosity, which is difficult to measure through experimentation (Decker et al., 1998; Tranter et al., 2019; Zare and Hashemabadi, 2019). Compared with the former techniques, direct determination of path length is possible when image analysis or other related methods are applied (San Wu et al., 2006).

In addition to directly measuring tortuosity, image analysis has other benefits, such as measuring tortuosity at different positions and in different directions on the structure. It is also worth mentioning that the use of image analysis for tortuosity measurement can visualize the path found and make the concept of tortuosity more perceptible (San Wu et al., 2006; Tranter et al., 2019). Another important way to estimate the tortuosity is using the results from dissolution measurements, which is an indirect technique. In this way, tortuosity can be estimated from some parameters related to the dissolution of a matter out of a matrix (Desai et al., 1965; Huang et al., 2019; San Wu et al., 2006; Shen and Chen, 2007). Tortuosity can also be measured using diffusion coefficients and porosity obtained from Nuclear magnetic resonance measurements (San Wu et al., 2006).

Agent-based modeling (ABM) is a powerful, fundamental, distributed artificial intelligence-based technique used to model and simulate complex systems through interactions among patches and agents. ABM has been employed to solve mass transfer problems, such as diffusion, forward osmosis process (Taherian and Mousavi, 2017; Taherian et al., 2018), oil absorption, water evaporation (Ghaitaranpour et al., 2024; Ghaitaranpour et al., 2021), and flavor release (Zandi and Mohebbi, 2015) successfully because of its unique similarities with real-world. This new method of modeling can also be combined with image processing techniques and the main principle of diffusion (Brownian motion) to measure tortuosity.

The current method offers several advantages over traditional image processing techniques for estimating tortuosity, including the ability to

measure tortuosity in irregularly shaped materials. In this paper, we employ a two-dimensional agent-based model to identify the shortest path through the pores in bread images during baking and bread dough. By leveraging Brownian motion, the fundamental principle underlying diffusion phenomena, this agent-based model gives a very close approximation of the shortest path. Standard images, bread crumbs and bread dough during baking and fermentation were used as model systems. This new technique can be used to determine the tortuosity of materials with both regular and irregular geometric shapes, and study the influence of shape and distribution of cavities on the tortuosity value of porous materials.

2. Materials and methods

2.1. Materials

Wheat flour (Golha food industries, Tehran, Iran), Sugar (Golestan, Tehran, Tehran, Iran), Sunflower oil (Kourosh food industry, Karaj., Alborz, Iran), instant dried yeast (Razavi yeast Co. Mashhad, Khorasan Razavi, Iran), and salt (Golha food industries, Tehran, Iran) was purchased from the local market before the experiments.

2.2. Preparation of bread samples

Bread dough was prepared according to the method given by Jafari et al. (2018) with some modifications. In brief, the dough preparation process has two main steps; In the first one, solid and liquid ingredients composed of wheat flours (60%), water (30%), sunflower oil (4%), instant dried yeast (1.5%), sugar (3%) and salt (2.5%) were mixed and kneaded in a Huger mixer (model HG550TMEM, China) for 8 min. In the second phase, the dough was cut into 140 g pieces, and they were placed into the oven (35 °C and 80–85% relative humidity) for 110 min to complete the fermentation process. After the fermentation process, one sample was frozen quickly by liquid nitrogen and stored until further studies. Bread dough was baked at 200 °C. Baking time was 30 min, and samples were collected at four time points: 5, 10, 15 and 30 min during baking and frozen quickly by liquid nitrogen, and stored at −18 °C until further analyses.

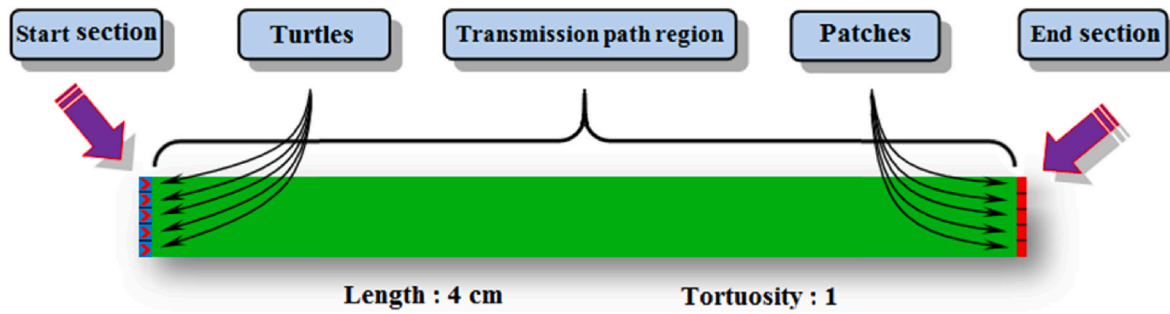


Fig. 2. Properties and components of a typical standard image to evaluate its tortuosity.

2.3. Image acquisition and preprocessing

2.3.1. Bread and bread dough images

Initially, a cross-sectional slice of frozen bread and bread dough was prepared with a sharp knife. To do that, the samples were cut perpendicular to the direction of Earth's gravity and stained blue using a brush to increase the color contrast between pores and walls surface. The images were taken by a specific lighting system detailed in our previous study (Ghaitaranpour et al., 2017). The sample images were taken with a digital camera (EOS 1000D; Canon, Tokyo, Japan) and imported to ImageJ software (1.6.0_05). Images were converted to 8-byte type, and then, pores, wall, and background were detected using the Otsu method (Fig. 1). Noises of images were removed by applying morphological operations (dilation and erosion). Finally, the preprocessed image was imported into NetLogo software and used for further analysis (Ghaitaranpour et al., 2020).

2.3.2. Standard images

To investigate the accuracy and validity of the current method in estimating the tortuosity of real materials, some standard images were designed by paint software (version 6.3) and saved in the PNG format (1800 × 800 pix). As shown in Fig. 2, each standard image has three connected parts named start section, transmission path region, and end section. They also have a predefined length and tortuosity.

2.4. Porosity evaluation of bread and bread dough

The samples with dimensions of 60 × 27 mm² were cut from the central region of sliced bread or bread dough. The porosity of each sample was measured by following equation (2) through calculating the difference between the solid phase surface (S_{PS}) and the total surface of the sample (t_{ss}) as mentioned below (Ghaitaranpour et al., 2018a,b) and the reported result represents the mean value calculated from a minimum of three replications:

$$\text{Total porosity} = \frac{t_{ss} - S_{PS}}{t_{ss}} \quad (2)$$

2.5. Calculation of average tortuosity

2.5.1. Principles and algorithm development

The transmission path region length was measured using the binary images of the desired part of the material. A two phase-system (A binary image) is more similar to the physical structure of porous substance (consisting of either pore phase and solid phase) compared with a gray-scale image (San Wu et al., 2006). The path length was calculated using the "principle of diffusion phenomena," applied in numerous unit operations such as dissolution, drying, and osmosis. This new algorithm detects the path related to the shortest traveling time of turtles (agents) when they go from a group of predefined patches in the start section to any other patches in the end section of the image. As mentioned before, this shortest path is determined using the main principle of diffusion,

which is called "Brownian motion." It is a random motion of tiny particles, significantly smaller than one μm suspended in a liquid or a gas caused by their collision with the other molecules of the fluid medium or the container's edge (Hao, 2011; Tranter et al., 2019).

The start and end sections of a path can be divided into some sub-sections called patches. In Fig. 2, each one was divided into 5 patches. Five agents (turtles) as a symbol of tiny particles are located in the starting patches that want to reach the end section follow Brownian motion principles (Fig. 2). The required number of turtles in each starting patch depends on the image's dimensions and complexity, i.e., bigger images need more turtles than smaller ones. There was just one turtle on any starting patch in our first experiment, which increased step by step until the time needed to reach the first turtle from each starting patch to the end section became constant.

This was done to study the impact of the ratio of turtles' number to the number of the starting patches (RTN) on the resulting path length. In the following path length estimation, a RTN of 5000 for standard images and 6000 for bread and bread dough were chosen because of the finding that raising the number of turtles any further did not change the path found, as will be discussed later.

Setting the number of turtles, the shortest path through the pores of standard and authentic images (bread and bread dough) could be estimated. All the patches on one side of the actual image of bread and bread dough were defined as start sections for the paths, and all the patches on the other side of the image were considered the end section. Standard and actual images resulted in 5 and 80 path lengths respectively from one end to another based on the length of considered start section for each image. From these path lengths, the average tortuosity of samples was computed using equation (3):

$$\bar{\tau} = \frac{\sum_{i=1}^n X_{Path}}{\sum_{i=1}^n X_{Image}} \quad (3)$$

in which $\bar{\tau}$ is the average tortuosity of the image, n is the number of starting patches. X_{Path} is the length of the shortest path in pores between the start and the end patch of the image while X_{Image} is the Euclidean distance between those two points. These procedures were done for both the standard and real images. Equation (3) should be rewritten considering our algorithm in this study to be processed by NetLogo. In this algorithm, the required time needed to travel from the start section to another end by each turtle (which are moving with predefined velocity) is measured instead of measuring the distance directly, so equation (3) is rewritten as follows:

$$X_{Path} = V \times t_{Path} \quad (4)$$

$$X_{Image} = V \times t_{Image} \quad (5)$$

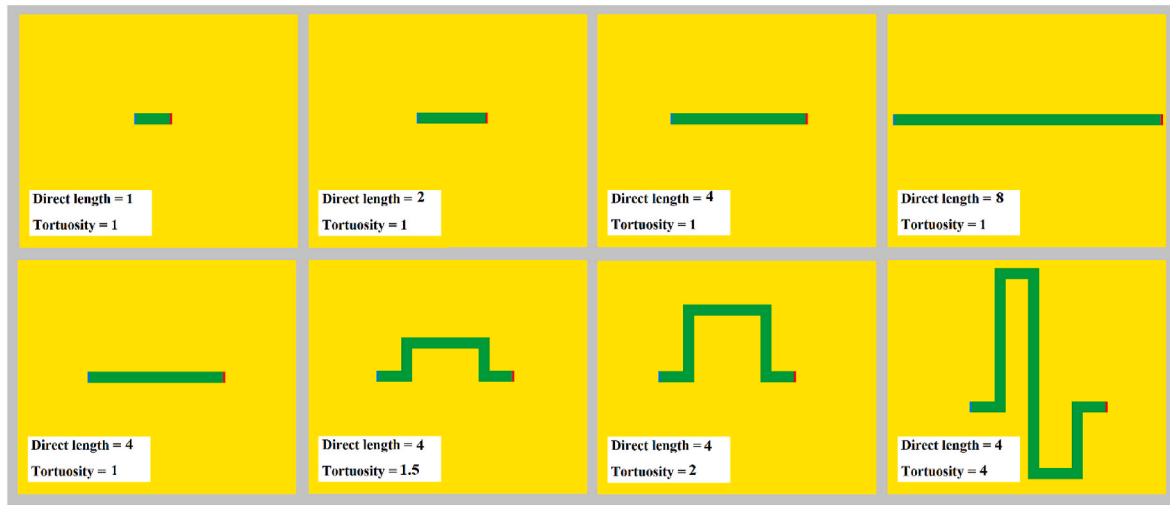


Fig. 3. Standard images with different predefined tortuosity and direct lengths used for method calibration.

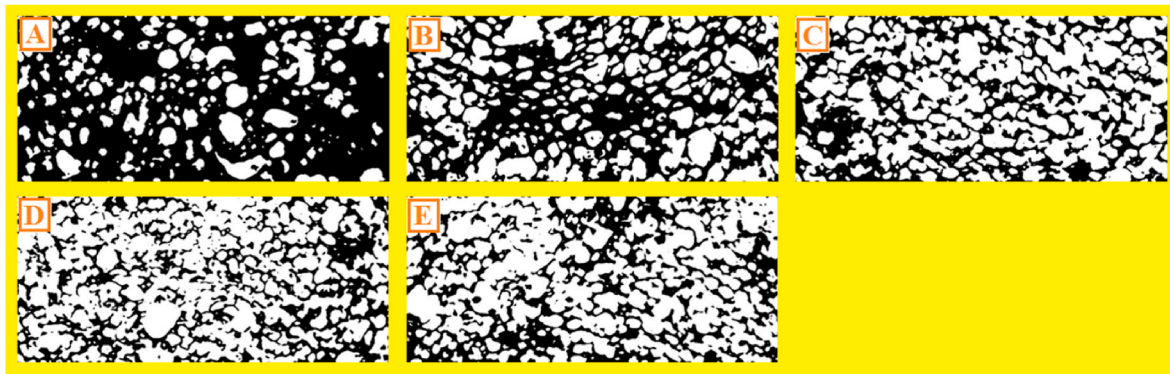


Fig. 4. The internal structure of bread and bread dough. A: bread dough, B, C, D & E: Bread after 5, 10, 15 and 30 min of baking process, respectively.

$$\bar{\tau} = \frac{\sum_{i=1}^n (V \times t_{pathi})}{\sum_{i=1}^n (V \times t_{imagei})} = \frac{\sum_{i=1}^n t_{pathi}}{\sum_{i=1}^n t_{imagei}} \quad (6)$$

in which V is the predefined velocity, n is the number of starting patches, t_{pathi} is the required time for passing the distance between the start section and end section as presented by each image, and t_{imagei} is the required time to pass the length or width of the image directly.

Typical running times were about 2 min on a standard computer. By considering all the time needed to reach the end section by the first turtle of each starting patch and averaging them, the average time needed to pass through the image is found. Dividing this average time by the time needed to pass the image length or width directly results in the average tortuosity. The standard deviation for obtained tortuosity was calculated based on the minimum time required for turtles to travel from each starting point to the endpoint. This procedure was carried out in Netlogo for each image of the samples.

2.5.2. Average tortuosity of standard images

Fig. 3 shows eight standard images with predefined length and tortuosity used for performance evaluation and standardization of the new method of tortuosity estimation, which is considered in current article. As can be seen from the figure, standard images of the first row have the same tortuosity, but their direct length increases from left to right. In the second row, the direct length of images is constant (4 cm) while their tortuosity increases from 1 to 4.

2.5.3. Average tortuosity of bread and bread dough

Fig. 4 shows the image of real samples used to measuring tortuosity by our developed algorithm. The first row images are related to the fermentation process of bread dough, while the second row illustrates the structural changes of dough as affected by the baking process. Processing time in both the first and second row increases from left to right.

2.6. Heterogeneity evaluation

The standard deviation of minimum arrival time (SDMT) is a measure of the amount of variation or dispersion of the minimum time needed for at least one turtle of each starting patch to go to the end patch. A low standard deviation indicates that the values tend to be close to the mean of the set and structure of material is more or less homogeneous, while a high standard deviation indicates that the values are spread out over a wider range and there is a considerable amount of heterogeneity in the material's structure. The SDMT was computed using equation (7):

$$SDMT = \sqrt{\frac{\sum_{i=1}^n (t_{pathi} - t_m)^2}{n}} \quad (7)$$

in which t_m is the average required time for passing the distance between the start section and end section for all paths in the desired direction, t_{pathi} is the shortest time for passing the length of one path, n is the number of starting patches.

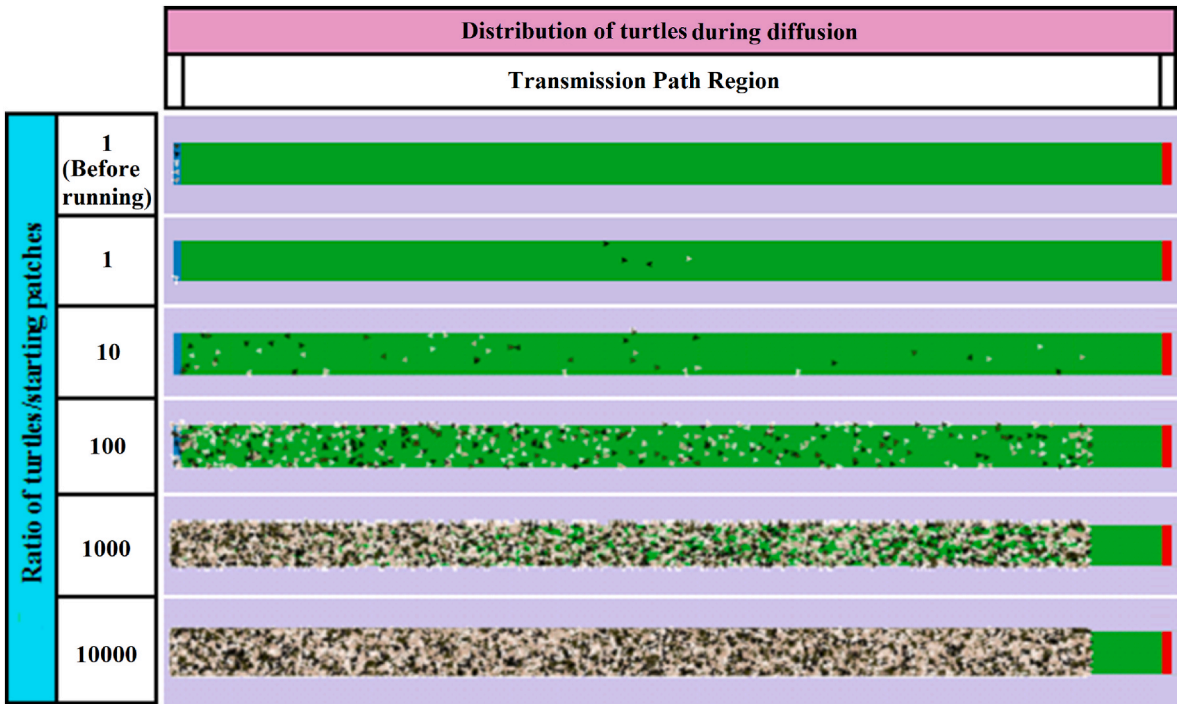


Fig. 5. Distribution of turtles based on principles of Brownian motion after 450 s of model execution.

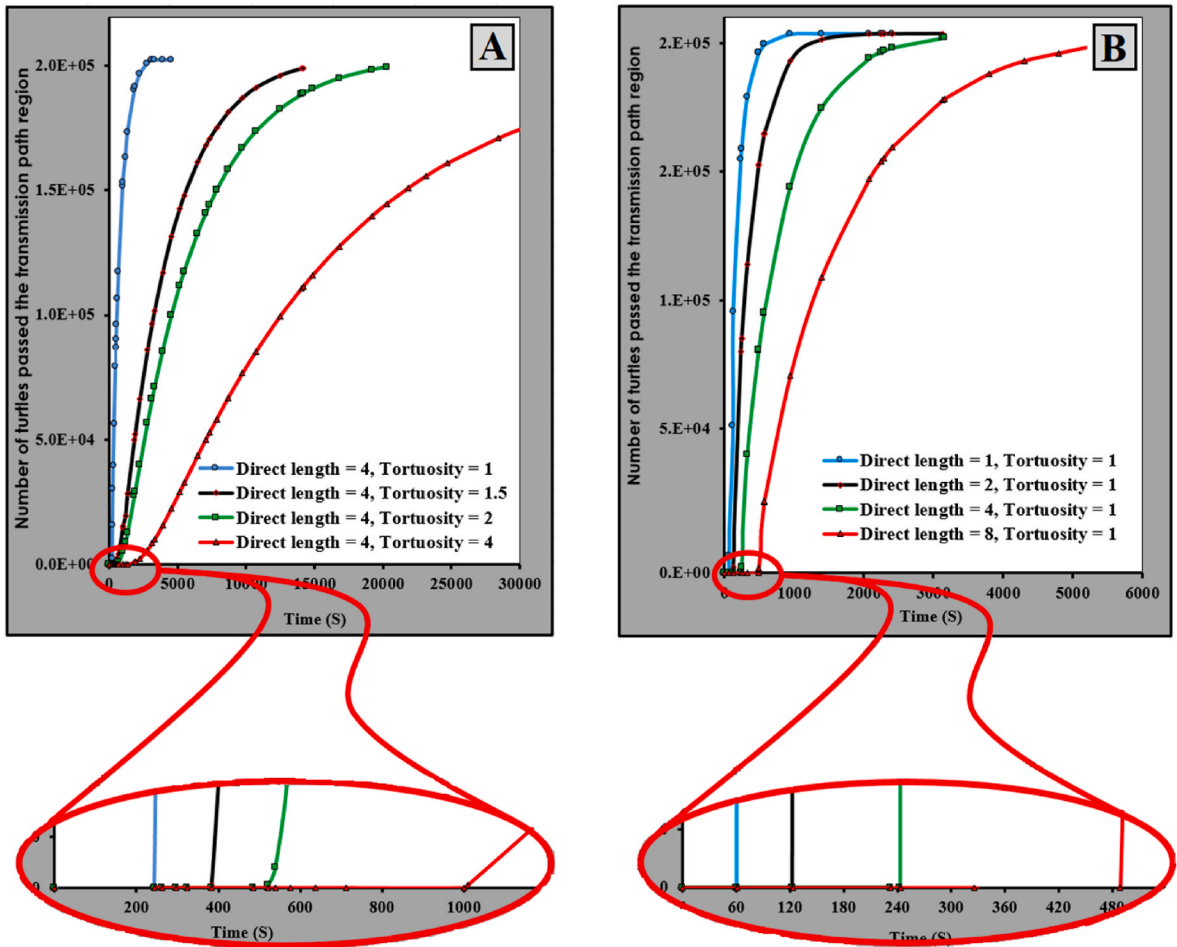


Fig. 6. The influence of direct length and tortuosity of standard images on the minimum time required to traverse the transmission path region. A: Images with tortuosity = 1 and varying direct lengths. B: Images with a direct length = 4 and varying tortuosity.

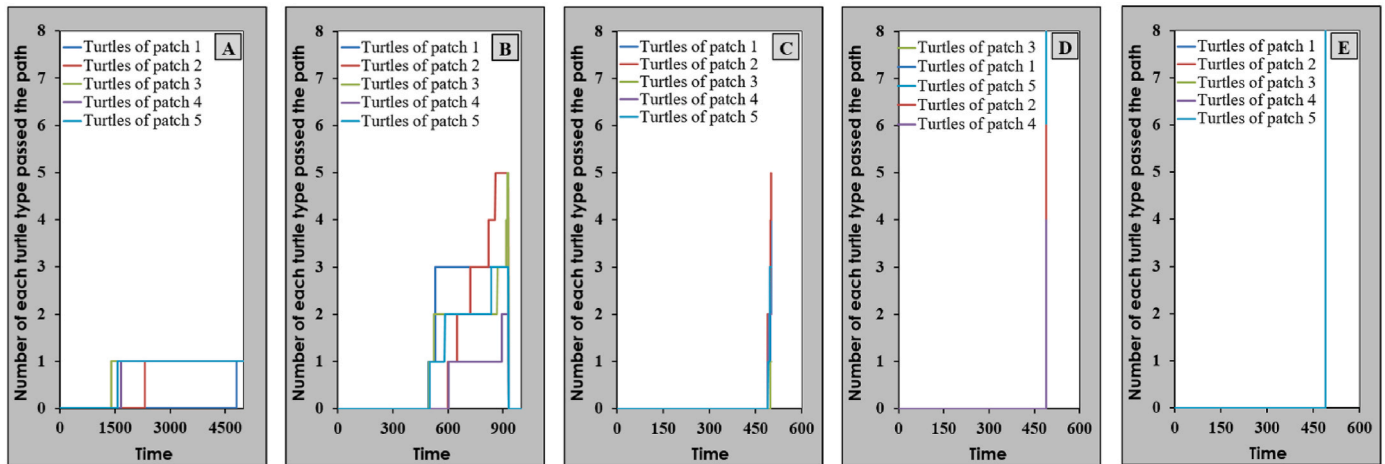


Fig. 7. Effect of RTN (1, 10, 100, 1000, 10000 for A, B, C, D and E respectively) on the minimum time needed to pass the transmission path region.

3. Results and discussion

3.1. Influence of difference in RTN on the pattern of turtles distribution

The principle of Brownian motion by different RTN and pattern of turtles distribution is demonstrated in Fig. 5. This figure shows the difference in the propagation pattern of turtles and the formation of the turtle's front propagation in the transmission path region.

For visualization purposes, the turtle's number per starting patch was set to 1, 10, 100, 1000, 10000 in different typical standard images. As shown in Fig. 5 the turtle's front formation and propagation in the transmission path region are much more visible in many turtles than in the smaller ones. After determination of the shortest path from all starting patches in the start section to at list one patch in the end section of the image by the principle of diffusion (Brownian motion), the minimum time needed for at least one turtle of each starting patch to go to the end patch was calculated.

3.2. Effect of tortuosity and direct length on diffusion pattern of turtles in standard images

Fig. 6 shows the effect of standard image properties on the diffusion pattern. Simulation of diffusion in a channel shows three connected steps named beginning step (shown by a red oval in Fig. 6), main step, and end step.

For very long or very tortuous path (Fig. 6, red curves), the expected shortest time is slightly overestimated.

Direct length and tortuosity of standard images had an obvious effect on all the mentioned three steps. As illustrated in Fig. 6, there is a linear relationship between the first step and features of standard images (direct length and tortuosity) used in the current work. Fig. 6A shows that as the direct length of images rises, the minimum time needed to pass the transmission path region in the first step increases proportionally. The same manner can be observed in the case of an increase in tortuosity of the images (Fig. 6B). The effect of an increase in tortuosity is more obvious because it also had a strong effect on the slope of the curve at the beginning step.

3.3. Influence of difference in RTN on average tortuosity

Comparison of Fig. 7A with B, C, D & E shows that there is an influence of RTN on the minimum time needed to pass the transmission path region. For this experiment, the RTN was from 1 to 10000. Fig. 7 shows the minimum time needed to pass the transmission path region as a function of the RTN to elevation a standard image with a direct length of 8 and tortuosity of 1. The relationship between RTN and the minimum

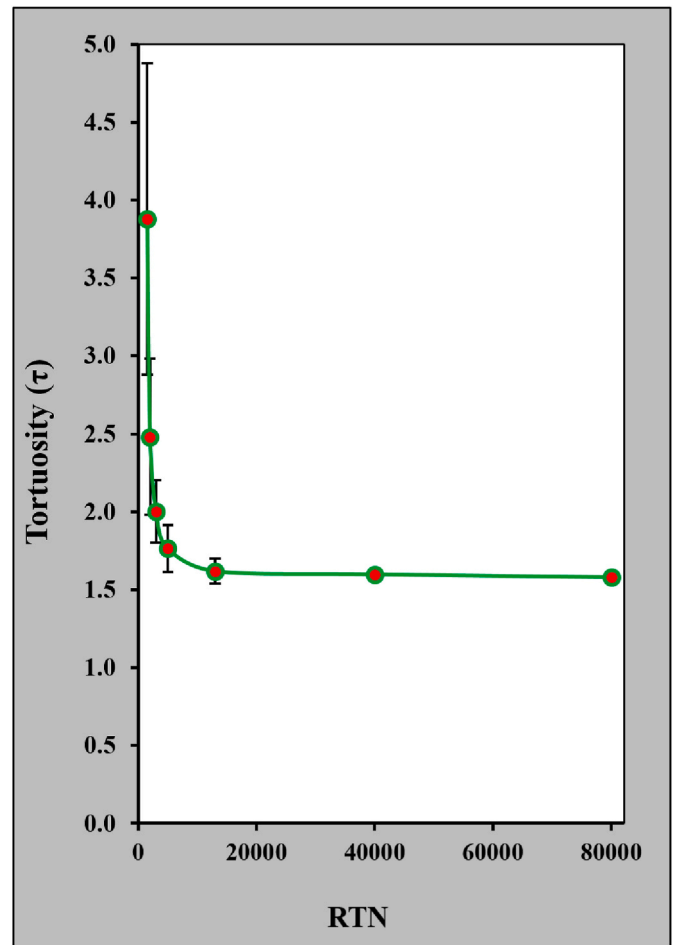


Fig. 8. Effect of RTN on the estimation of tortuosity value of the standard images with direct length and tortuosity of 4 & 1.5 respectively.

time needed to pass the transmission path region is similar for the other images.

Fig. 7 shows that the minimum time needed to pass the transmission path region decreases with increasing RTN until a certain minimum is reached. This can be described as follows: when RTN is small, the turtle's front propagation is not completely formed. Therefore, there are not enough turtles to find the shortest path in the least possible time.

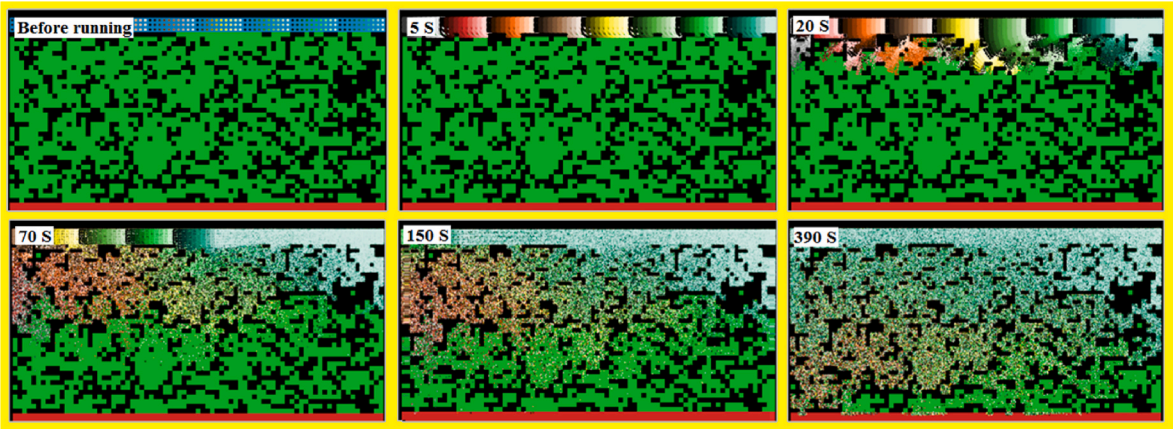


Fig. 9. The spatial distribution of turtles at various time intervals during model execution.

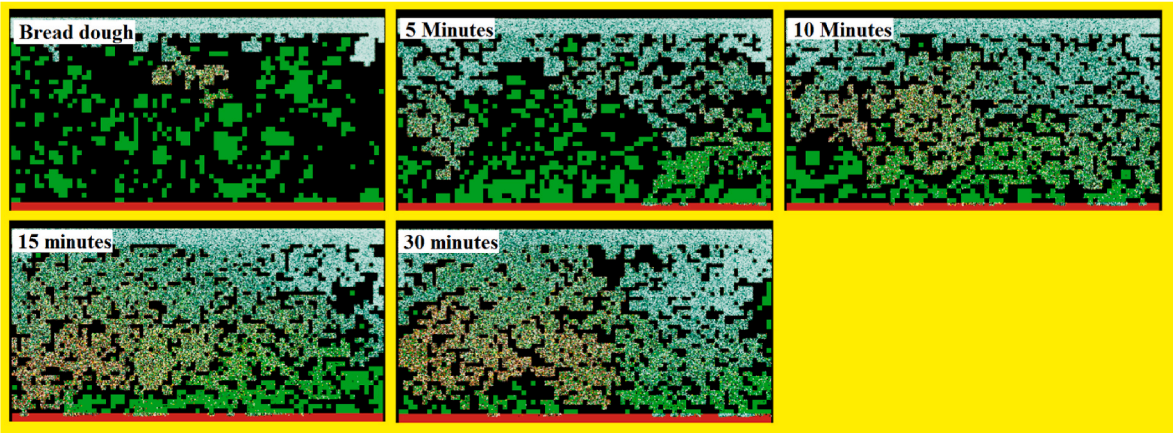


Fig. 10. Effect of baking time on the turtle’s diffusion in the internal structure of bread and bread dough during baking.

However, when the RTN is larger, it is faster to find a way to the other side of the picture; this decreases the average tortuosity, as is illustrated in Figs. 5 and 7. Above certain RTN, the minimum time needed to pass the transmission path region remains the same, and therefore the average tortuosity reaches an asymptotic value as shown in Fig. 8. Consequently, the number of turtles is insufficient to identify the shortest path in the least possible time, as demonstrated by the significant variation in the time taken for turtles to find the shortest path from the starting point to the endpoint (Fig. 7A). The error bars for different RTNs was calculated using these variations and is presented in Fig. 8.

3.4. Penetration of turtles into the structure of bread crumb as a transmission path region

Fig. 9 illustrates how turtles penetrate the bread structure and find connected pores based on principles of Brownian motion to go from one side of the picture to another side while running the developed algorithm.

As shown in Figs. 9 and 10, turtles located on each patch of start section begin to penetrate the nearest pores, but they cover all pores connected to the start section while running the algorithm. It can help the turtles to find the shortest path between two opposite sides of the image in the shortest time.

3.5. Influence of baking time on the porosity and tortuosity of internal dough structure

To minimize the path length through the pore phase as a

Table 1			
Porosity, tortuosity and SDT of samples.			
Sample type	Porosity (%)	Tortuosity	SDT
Standard image	100	1	0
Bread dough	37.1 ± 11.9	∞	–
Bread after 5 min baking	47.7 ± 4.3	16.3 ± 4.2	462.8
Bread after 10 min baking	60.8 ± 4.9	4.6 ± 1.2	120.5
Bread after 15 min baking	61.1 ± 8.9	2.0 ± 0.6	58.5
Bread after 30 min baking	60.9 ± 6.4	2.4 ± 0.7	65.8

transmission path region, the RTN has been set to 5000 turtles/starting path. Comparison of different parts of Fig. 10 shows that there is an influence of porosity on the depth of the turtle’s penetration in the structure of bread and bread dough. The turtle’s diffusion through the pores in the transects images is higher for the cores containing large connected pores compared with the low porosity ones.

Researchers reported that bread dough volume change follows a unique manner during baking (Zhang and Datta, 2006). Different types of bread images show a rapid increase in volume at the initial stages of baking, followed by a decrease and stabilization at the final parts of the process (Babin et al., 2006; Zhang and Datta, 2006).

Our findings, as presented in Table 1, agree with other researchers’ statements about bread porosity during baking(Nicolas et al., 2016; Zhang and Datta, 2006). Results showed that the tortuosity of the internal structure of bread changed during baking. Table 1 and Fig. 9 show a positive correlation between tortuosity and porosity of bread crumbs (Zare and Hashemabadi, 2019). Baking time had a significant impact (p

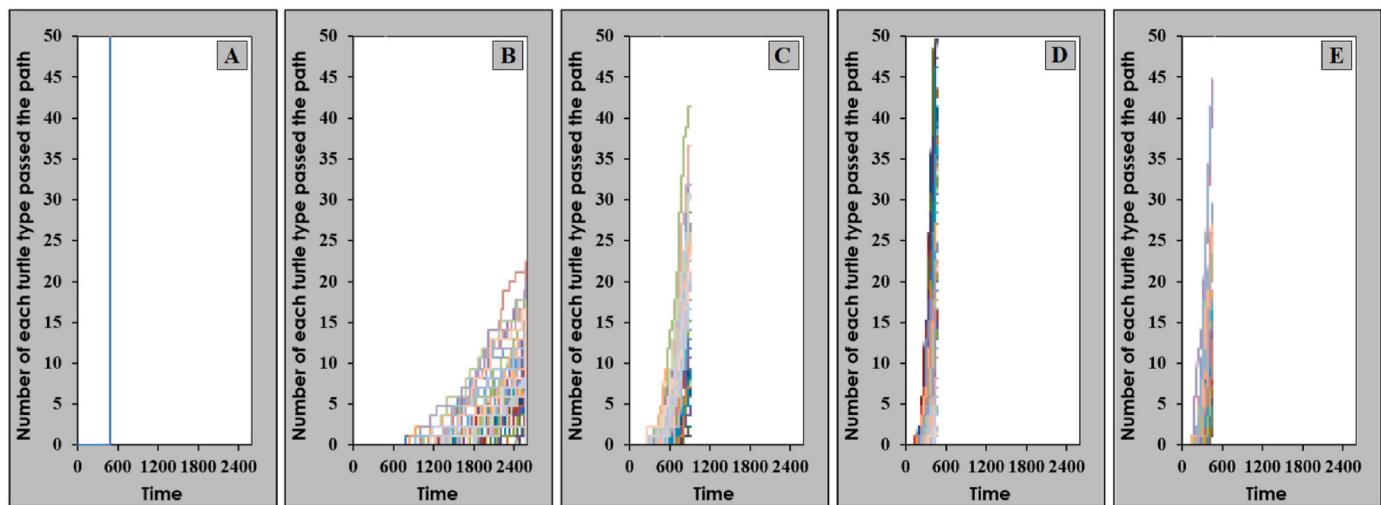


Fig. 11. Effect of structural heterogeneity on the minimum time needed to pass the transmission path region. A: standard image. B, C, D & E: bread dough after 5, 10, 15 and 30 min baking, respectively.

< 0.05) on the tortuosity of bread samples. During the initial 15 min of baking, tortuosity decreased continuously. This observation can be attributed to the continuous increase in bread porosity within the specified time frame. As the bread bakes, air bubbles expand, and some of them merge, ultimately creating shorter paths through the bread structure. However, a slight decrease was observed during the final 5 min of baking, likely due to changes in bread porosity. This result follows the finding of other researchers about the relation between porosity and tortuosity (Shen and Chen, 2007; Tranter et al., 2019; Zare and Hashemabadi, 2019). They stated that as the porosity increases, the value of the tortuosity decreases following various mathematical formulas to evaluate different types of case studies. The accuracy of our approach is largely sufficient to correctly probe the change of tortuosity during baking.

The tortuosity of cellular structure of bread crumb has also been investigated by other scientists using gray-weighted distance transform (Besbes et al., 2013). They states that this parameter is between 1.17 and 1.61 for different directions and processing conditions after 20 min of backing. The finding of the current study is higher than what had been reported about bread by other researchers (Besbes et al., 2013). It is because of the fact that in our study, the porosity of samples were about 60%, which is only two third of porosity of samples with lower tortuosity (Besbes et al., 2013).

3.6. Structural heterogeneity

Figs. 3 and 4 show examples of standard images and also bread images during the baking process. All bread images are taken from the porous structure of the crumb. Visual observation of these figures reveals a difference in structure. There was not any heterogeneity in the transmission path region of standard images, while the bread images did not have a uniform structure. This is in concurrence with results found by other researchers who observed heterogeneity in the structure of cross-sectional images of various types of bread (Rathnayake et al., 2018); However, they did not introduce a procedure of heterogeneity measurement of crumb structure. Fig. 11 describes the minimum time needed to pass the transmission path region.

The SDMT provides a method of analyzing heterogeneity in structure since the heterogeneity in structure shows that the path length through the pores in a special part of the material is different from other parts. Indeed, the SDMT measured in the standard images, is equal to zero, significantly shorter than in the bread images when measured through the pore phase as a transmission path region, as shown in Figs. 8 and 11 and Table 1. This was also observed in bread images during baking,

suggesting that the SDMT provides a useful measure to evaluate the heterogeneity of different structures.

4. Conclusion

An agent-based two-dimensional method presented in this work was used successfully to estimate the average tortuosity in images of cross sectional-slice of bread and bread dough. One of the main contributions of this method is the addition of Brownian motion principles to the tortuosity estimation procedure, inspired by the real situation existing in phenomena such as diffusion. By exploiting the full distribution of sojourn times, ABM could also give easily information related to transport by diffusion such as mean residence time. This study showed that baking time has an obvious effect on the tortuosity of bread's porous structure. In the first stage of baking, tortuosity decreased dramatically while at the end of this process, the tortuosity of the bread structure increased slightly. Additionally, the effect of porosity and pore distribution pattern on tortuosity could be easily estimated, and heterogeneity of the structure could be illustrated. Therefore, the proposed method is an important way to estimate tortuosity, which has several applications in food science, particularly in understanding and controlling the properties of food materials and their behavior during processing like drying, storage, and consumption. It can also be useful in the study of transport phenomena, especially mass transfer, in porous material.

CRediT authorship contribution statement

Arash Ghaitaranpour: Conceptualization, Data curation, Investigation, Formal analysis, Validation, Visualization, Writing – original draft. **Mohebbat Mohebbi:** Funding acquisition, Methodology, Project administration, Resources, Software, Supervision. **Arash Koocheki:** Supervision, Writing – review & editing.

Declaration of competing interest

The authors declare that they have no known competing financial interests or personal relationships that could have appeared to influence the work reported in this paper.

Acknowledgments

The authors would like to thank the Deputy of Research and Technology of the Ferdowsi University of Mashhad for financial support.

Special thanks to Dr. Kordiyeh Hamidi Loyen for her technical support given to this research.

Data availability

Data will be made available on request.

References

- Abderrahmene, M., Abdelillah, B., Fouad, G., 2017. Electrical prediction of tortuosity in porous media. *Energy Proc.* 139, 718–724.
- Babin, P., Della Valle, G., Chiron, H., Cloetens, P., Hoszowska, J., Pernot, P., Réguerre, A., Salvo, L., Dendievel, R., 2006. Fast X-ray tomography analysis of bubble growth and foam setting during breadmaking. *J. Cereal. Sci.* 43 (3), 393–397.
- Besbes, E., Jury, V., Monteau, J.Y., Le Bail, A., 2013. Characterizing the cellular structure of bread crumb and crust as affected by heating rate using X-ray microtomography. *J. Food Eng.* 115 (3), 415–423.
- Decker, L., Jeulin, D., Toven, I., 1998. 3D morphological analysis of the connectivity of a porous medium *Acta Stereologica*, 17 (1), 107–112.
- Desai, S., Simonelli, A., Higuchi, W., 1965. Investigation of factors influencing release of solid drug dispersed in inert matrices. *J. Pharmaceut. Sci.* 54 (10), 1459–1464.
- Ghaitaranpour, A., Koocheki, A., Mohebbi, M., 2024. Simulation of bread baking with a conceptual agent-based model: an approach to study the effect of proofing time on baking behavior. *J. Food Eng.* 368, 111920.
- Ghaitaranpour, A., Koocheki, A., Mohebbi, M., Ngadi, M.O., 2018a. Effect of deep fat and hot air frying on doughnuts physical properties and kinetic of crust formation. *J. Cereal. Sci.* 83, 25–31.
- Ghaitaranpour, A., Mohebbi, M., Koocheki, A., 2018b. Characterizing the cellular structure of air and deep fat fried doughnut using image analysis techniques. *J. Food Eng.* 237, 231–239.
- Ghaitaranpour, A., Mohebbi, M., Koocheki, A., 2021. An innovative model for describing oil penetration into the doughnut crust during hot air frying. *Food Res. Int.* 147, 110458.
- Ghaitaranpour, A., Mohebbi, M., Koocheki, A., Ngadi, M.O., 2020. An agent-based coupled heat and water transfer model for air frying of doughnut as a heterogeneous multiscale porous material. *Innov. Food Sci. Emerg. Technol.*, 102335.
- Ghaitaranpour, A., Rastegar, A., Tabatabaei Yazdi, F., Mohebbi, M., Alizadeh Behbahani, B., 2017. Application of digital image processing in monitoring some physical properties of tarkhineh during drying. *J. Food Process. Preserv.* 41 (2), e12861.
- Ghanbarian, B., Hunt, A.G., Ewing, R.P., Sahimi, M., 2013. Tortuosity in porous media: a critical review. *Soil Sci. Soc. Am. J.* 77 (5), 1461–1477.
- Hao, T., 2011. *Electrorheological Fluids: the Non-aqueous Suspensions*, vol. 22. Elsevier.
- Huang, J., Xiao, F., Dong, H., Yin, X., 2019. Diffusion tortuosity in complex porous media from pore-scale numerical simulations. *Comput. Fluid* 183, 66–74.
- Jafari, M., Koocheki, A., Milani, E., 2018. Physicochemical and sensory properties of extruded sorghum–wheat composite bread. *J. Food. Meas. Charact.* 12, 370–377.
- Kuruneru, S.T., Sauret, E., Vafai, K., Saha, S.C., Gu, Y., 2017. Analysis of particle-laden fluid flows, tortuosity and particle-fluid behaviour in metal foam heat exchangers. *Chem. Eng. Sci.* 172, 677–687.
- Martin, A., 1993. *Physical Pharmacy: Physical Chemical Principles in the Pharmaceutical Sciences*: BI Waverly. Pvt Ltd.
- Nicolas, V., Vanin, F., Grenier, D., Lucas, T., Doursat, C., Flick, D., 2016. Modeling bread baking with focus on overall deformation and local porosity evolution. *AIChE J.* 62 (11), 3847–3863.
- Rathnayake, H., Navaratne, S., Navaratne, C., 2018. Porous crumb structure of leavened baked products. *Int. J. Food Sci.* 2018.
- San Wu, Y., van Vliet, L.J., Frijlink, H.W., van der Voort Maarschalk, K., 2006. The determination of relative path length as a measure for tortuosity in compacts using image analysis. *Eur. J. Pharmaceut. Sci.* 28 (5), 433–440.
- Shen, L., Chen, Z., 2007. Critical review of the impact of tortuosity on diffusion. *Chem. Eng. Sci.* 62 (14), 3748–3755.
- Silva, J.V.C., Lortal, S., Floury, J., 2015. Diffusion behavior of dextrans in dairy systems of different microstructures. *Food Res. Int.* 71, 1–8.
- Taherian, M., Mousavi, S.M., 2017. Modeling and simulation of forward osmosis process using agent-based model system. *Comput. Chem. Eng.* 100, 104–118.
- Taherian, M., Mousavi, S.M., Chamani, H., 2018. An agent-based simulation with NetLogo platform to evaluate forward osmosis process (PRO Mode). *Chin. J. Chem. Eng.* 26 (12), 2487–2494.
- Tranter, T., Kok, M., Lam, M., Gostick, J., 2019. pytrax: a simple and efficient random walk implementation for calculating the directional tortuosity of images. *SoftwareX* 10, 100277.
- Zandi, M., Mohebbi, M., 2015. An agent-based simulation of a release process for encapsulated flavour using the NetLogo platform. *Flavour Fragrance J.* 30 (3), 224–229.
- Zare, M., Hashemabadi, S.H., 2019. CFD simulation and experimental validation of tortuosity effects on pellet-fluid heat transfer of regularly stacked multi-lobe particles. *Chem. Eng. J.* 361, 1543–1556.
- Zhang, J., Datta, A., 2006. Mathematical modeling of bread baking process. *J. Food Eng.* 75 (1), 78–89.